Directed flow in Au+Au collisions at $\sqrt{s_{NN}} = 62.4$ GeV

J. Adams,[3] M. M. Aggarwal,[29] Z. Ahammed,[44] J. Amonett,[20] B. D. Anderson,[20] D. Arkhipkin,[13] G. S. Averichev,[12] S. K. Badyal,[19] Y. Bai,[27] J. Balewski,[17] O. Barannikova,[32] L. S. Barnby,[3] J. Baudot,[18] S. Bekele,[28] V. V. Belaga,[12] A. Bellingeri-Laurikainen,[39] R. Bellwied,[47] J. Berger,[14] B. I. Bezverkhny,[49] S. Bharadwaj,[34] A. Bhasin,[19] A. K. Bhati,[29] V. S. Bhatia,[29] H. Bichsel,[46] J. Bielcik,[49] J. Bielcikova,[49] A. Billmeier,[47] L. C. Bland,[4] C. O. Blyth,[3] S.-L. Blyth,[21] B. E. Bonner,[35] M. Botje,[27] A. Boucham,[39] J. Bouchet,[39] A. V. Brandin,[25] A. Bravar,[4] M. Bystersky,[11] R. V. Cadman,[1] X. Z. Cai,[38] H. Caines,[49] M. Calderón de la Barca Sánchez,[17] J. Castillo,[21] O. Catu,[49] D. Cebra,[7] Z. Chajecki,[28] P. Chaloupka,[11] S. Chattopadhyay,[44] H. F. Chen,[37] J. H. Chen,[38] Y. Chen,[8] J. Cheng,[42] M. Cherney,[10] A. Chikanian,[49] H. A. Choi,[33] W. Christie,[4] J. P. Coffin,[18] T. M. Cormier,[47] M. R. Cosentino,[36] J. G. Cramer,[46] H. J. Crawford,[6] D. Das,[44] S. Das,[44] M. Daugherity,[41] M. M. de Moura,[36] T. G. Dedovich,[12] M. DePhillips,[4] A. A. Derevschikov,[31] L. Didenko,[4] T. Dietel,[14] S. M. Dogra,[19] W. J. Dong,[8] X. Dong,[37] J. E. Draper,[7] F. Du,[49] A. K. Dubey,[15] V. B. Dunin,[12] J. C. Dunlop,[4] M. R. Dutta Mazumdar,[44] V. Eckardt,[23] W. R. Edwards,[21] L. G. Efimov,[12] V. Emelianov,[25] J. Engelage,[6] G. Eppley,[35] B. Erazmus,[39] M. Estienne,[39] P. Fachini,[4] J. Faivre,[18] R. Fatemi,[22] J. Fedorisin,[12] K. Filimonov,[21] P. Filip,[11] E. Finch,[49] V. Fine,[4] Y. Fisyak,[4] K. S. F. Fornazier,[36] J. Fu,[42] C. A. Gagliardi,[40] L. Gaillard,[3] J. Gans,[49] M. S. Ganti,[44] F. Geurts,[35] V. Ghazikhanian,[8] P. Ghosh,[44] J. E. Gonzalez,[8] H. Gos,[45] O. Grachov,[47] O. Grebenyuk,[27] D. Grosnick,[43] S. M. Guertin,[8] Y. Guo,[47] A. Gupta,[19] N. Gupta,[19] T. D. Gutierrez,[7] T. J. Hallman,[4] A. Hamed,[47] D. Hardtke,[21] J. W. Harris,[49] M. Heinz,[2] T. W. Henry,[40] S. Hepplemann,[30] B. Hippolyte,[18] A. Hirsch,[32] E. Hjort,[21] G. W. Hoffmann,[41] M. J. Horner,[21] H. Z. Huang,[8] S. L. Huang,[37] E. W. Hughes,[5] T. J. Humanic,[28] G. Igo,[8] A. Ishihara,[41] P. Jacobs,[21] W. W. Jacobs,[17] M. Jedynak,[45] H. Jiang,[8] P. G. Jones,[3] E. G. Judd,[6] S. Kabana,[2] K. Kang,[42] M. Kaplan,[9] D. Keane,[20] A. Kechechyan,[12] V. Yu. Khodyrev,[31] B. C. Kim,[33] J. Kiryluk,[22] A. Kisiel,[45] E. M. Kislov,[12] J. Klay,[21] S. R. Klein,[21] D. D. Koetke,[43] T. Kollegger,[14] M. Kopytine,[20] L. Kotchenda,[25] K. L. Kowalik,[21] M. Kramer,[26] P. Kravtsov,[25] V. I. Kravtsov,[31] K. Krueger,[1] C. Kuhn,[18] A. I. Kulikov,[12] A. Kumar,[29] R. Kh. Kutuev,[13] A. A. Kuznetsov,[12] M. A. C. Lamont,[49] J. M. Landgraf,[4] S. Lange,[14] F. Laue,[4] J. Lauret,[4] A. Lebedev,[4] R. Lednicky,[12] C.-H. Lee,[33] S. Lehocka,[12] M. J. LeVine,[4] C. Li,[37] Q. Li,[47] Y. Li,[42] G. Lin,[49] S. J. Lindenbaum,[26] M. A. Lisa,[28] F. Liu,[48] H. Liu,[37] J. Liu,[35] L. Liu,[48] Q. J. Liu,[46] Z. Liu,[48] T. Ljubicic,[4] W. J. Llope,[35] H. Long,[8] R. S. Longacre,[4] M. Lopez-Noriega,[28] W. A. Love,[4] Y. Lu,[48] T. Ludlam,[4] D. Lynn,[4] G. L. Ma,[38] J. G. Ma,[8] Y. G. Ma,[38] D. Magestro,[28] S. Mahajan,[19] D. P. Mahapatra,[15] R. Majka,[49] L. K. Mangotra,[19] R. Manweiler,[43] S. Margetis,[20] C. Markert,[20] L. Martin,[39] J. N. Marx,[21] H. S. Matis,[21] Yu. A. Matulenko,[31] C. J. McClain,[1] T. S. McShane,[10] F. Meissner,[21] Yu. Melnick,[31] A. Meschanin,[31] M. L. Miller,[22] N. G. Minaev,[31] C. Mironov,[20] A. Mischke,[27] D. K. Mishra,[15] J. Mitchell,[35] B. Mohanty,[44] L. Molnar,[32] C. F. Moore,[41] D. A. Morozov,[31] M. G. Munhoz,[36] B. K. Nandi,[44] S. K. Nayak,[19] T. K. Nayak,[44] J. M. Nelson,[3] P. K. Netrakanti,[44] V. A. Nikitin,[13] L. V. Nogach,[31] S. B. Nurushev,[31] G. Odyniec,[21] A. Ogawa,[4] V. Okorokov,[25] M. Oldenburg,[21] D. Olson,[21] S. K. Pal,[44] Y. Panebratsev,[12] S. Y. Panitkin,[4] A. I. Pavlinov,[47] T. Pawlak,[45] T. Peitzmann,[27] V. Perevoztchikov,[4] C. Perkins,[6] W. Peryt,[45] V. A. Petrov,[47] S. C. Phatak,[15] R. Picha,[7] M. Planinic,[50] J. Pluta,[45] N. Porile,[32] J. Porter,[46] A. M. Poskanzer,[21] M. Potekhin,[4] E. Potrebenikova,[12] B. V. K. S. Potukuchi,[19] D. Prindle,[46] C. Pruneau,[47] J. Putschke,[21] G. Rakness,[30] R. Raniwala,[34] S. Raniwala,[34] O. Ravel,[39] R. L. Ray,[41] S. V. Razin,[12] D. Reichhold,[32] J. G. Reid,[46] J. Reinnarth,[39] G. Renault,[39] F. Retiere,[21] A. Ridiger,[25] H. G. Ritter,[21] J. B. Roberts,[35] O. V. Rogachevskiy,[12] J. L. Romero,[7] A. Rose,[21] C. Roy,[39] L. Ruan,[37] M. J. Russcher,[27] R. Sahoo,[15] I. Sakrejda,[21] S. Salur,[49] J. Sandweiss,[49] M. Sarsour,[40] I. Savin,[13] P. S. Sazhin,[12] J. Schambach,[41] R. P. Scharenberg,[32] N. Schmitz,[23] K. Schweda,[21] J. Seger,[10] I. Selyuzhenkov,[47] P. Seyboth,[23] E. Shahaliev,[12] M. Shao,[37] W. Shao,[5] M. Sharma,[29] W. Q. Shen,[38] K. E. Shestermanov,[31] S. S. Shimanskiy,[12] E. Sichtermann,[21] F. Simon,[22] R. N. Singaraju,[44] N. Smirnov,[49] R. Snellings,[27] G. Sood,[43] P. Sorensen,[21] J. Sowinski,[17] J. Speltz,[18] H. M. Spinka,[1] B. Srivastava,[32] A. Stadnik,[12] T. D. S. Stanislaus,[43] R. Stock,[14] A. Stolpovsky,[47] M. Strikhanov,[25] B. Stringfellow,[32] A. A. P. Suaide,[36] E. Sugarbaker,[28] M. Sumbera,[11] B. Surrow,[22] M. Swanger,[10] T. J. M. Symons,[21] A. Szanto de Toledo,[36] A. Tai,[8] J. Takahashi,[36] A. H. Tang,[27] T. Tarnowsky,[32] D. Thein,[8] J. H. Thomas,[21] A. R. Timmins,[3] S. Timoshenko,[25] M. Tokarev,[12] S. Trentalange,[8] R. E. Tribble,[40] O. D. Tsai,[8] J. Ulery,[32] T. Ullrich,[4] D. G. Underwood,[1] G. Van Buren,[4] N. van der Kolk,[27] M. van Leeuwen,[21] A. M. Vander Molen,[24] R. Varma,[16] I. M. Vasilevski,[13] A. N. Vasiliev,[31] R. Vernet,[18] S. E. Vigdor,[17] Y. P. Viyogi,[44] S. Vokal,[12] S. A. Voloshin,[47] W. T. Waggoner,[10] F. Wang,[32] G. Wang,[20] G. Wang,[5] X. L. Wang,[37] Y. Wang,[41] Y. Wang,[42] Z. M. Wang,[37] H. Ward,[41] J. W. Watson,[20] J. C. Webb,[17] G. D. Westfall,[24] A. Wetzler,[21] C. Whitten, Jr.,[8] H. Wieman,[21] S. W. Wissink,[17] R. Witt,[2] J. Wood,[8] J. Wu,[37] N. Xu,[21] Z. Xu,[4] Z. Z. Xu,[37] E. Yamamoto,[21] P. Yepes,[35] I.-K. Yoo,[33] V. I. Yurevich,[12] I. Zborovsky,[11] H. Zhang,[4] W. M. Zhang,[20] Y. Zhang,[37] Z. P. Zhang,[37] C. Zhong,[38] R. Zoulkarneev,[13] Y. Zoulkarneeva,[13] A. N. Zubarev,[12] and J. X. Zuo[38]

(STAR Collaboration)

[1]*Argonne National Laboratory, Argonne, Illinois 60439, USA*

[2]*University of Bern, 3012 Bern, Switzerland*

[3]*University of Birmingham, Birmingham, United Kingdom*

[4]*Brookhaven National Laboratory, Upton, New York 11973, USA*

[5]*California Institute of Technology, Pasadena, California 91125, USA*

[6]*University of California, Berkeley, California 94720, USA*

[7]*University of California, Davis, California 95616, USA*

 ©2006 The American Physical Society

[8]*University of California, Los Angeles, California 90095, USA*
[9]*Carnegie Mellon University, Pittsburgh, Pennsylvania 15213, USA*
[10]*Creighton University, Omaha, Nebraska 68178, USA*
[11]*Nuclear Physics Institute AS CR, 250 68 Řež/Prague, Czech Republic*
[12]*Laboratory for High Energy (JINR), Dubna, Russia*
[13]*Particle Physics Laboratory (JINR), Dubna, Russia*
[14]*University of Frankfurt, Frankfurt, Germany*
[15]*Institute of Physics, Bhubaneswar 751005, India*
[16]*Indian Institute of Technology, Mumbai, India*
[17]*Indiana University, Bloomington, Indiana 47408, USA*
[18]*Institut de Recherches Subatomiques, Strasbourg, France*
[19]*University of Jammu, Jammu 180001, India*
[20]*Kent State University, Kent, Ohio 44242, USA*
[21]*Lawrence Berkeley National Laboratory, Berkeley, California 94720, USA*
[22]*Massachusetts Institute of Technology, Cambridge, Massachusetts 02139-4307, USA*
[23]*Max-Planck-Institut für Physik, Munich, Germany*
[24]*Michigan State University, East Lansing, Michigan 48824, USA*
[25]*Moscow Engineering Physics Institute, Moscow Russia*
[26]*City College of New York, New York City, New York 10031, USA*
[27]*NIKHEF and Utrecht University, Amsterdam, The Netherlands*
[28]*Ohio State University, Columbus, Ohio 43210, USA*
[29]*Panjab University, Chandigarh 160014, India*
[30]*Pennsylvania State University, University Park, Pennsylvania 16802, USA*
[31]*Institute of High Energy Physics, Protvino, Russia*
[32]*Purdue University, West Lafayette, Indiana 47907, USA*
[33]*Pusan National University, Pusan, Republic of Korea*
[34]*University of Rajasthan, Jaipur 302004, India*
[35]*Rice University, Houston, Texas 77251, USA*
[36]*Universidade de Sao Paulo, Sao Paulo, Brazil*
[37]*University of Science & Technology of China, Anhui 230027, China*
[38]*Shanghai Institute of Applied Physics, Shanghai 201800, China*
[39]*SUBATECH, Nantes, France*
[40]*Texas A&M University, College Station, Texas 77843, USA*
[41]*University of Texas, Austin, Texas 78712, USA*
[42]*Tsinghua University, Beijing 100084, China*
[43]*Valparaiso University, Valparaiso, Indiana 46383, USA*
[44]*Variable Energy Cyclotron Centre, Kolkata 700064, India*
[45]*Warsaw University of Technology, Warsaw, Poland*
[46]*University of Washington, Seattle, Washington 98195, USA*
[47]*Wayne State University, Detroit, Michigan 48201, USA*
[48]*Institute of Particle Physics, CCNU (HZNU), Wuhan 430079, China*
[49]*Yale University, New Haven, Connecticut 06520, USA*
[50]*University of Zagreb, Zagreb, HR-10002, Croatia*

(Received 18 October 2005; published 8 March 2006)

We present the directed flow (v_1) measured in Au+Au collisions at $\sqrt{s_{NN}} = 62.4$ GeV in the midpseudorapidity region $|\eta| < 1.3$ and in the forward pseudorapidity region $2.5 < |\eta| < 4.0$. The results are obtained using the three-particle cumulant method, the event plane method with mixed harmonics, and for the first time at the Relativistic Heavy Ion Collider, the standard method with the event plane reconstructed from spectator neutrons. Results from all three methods are in good agreement. Over the pseudorapidity range studied, charged particle directed flow is in the direction opposite to that of fragmentation neutrons.

DOI: 10.1103/PhysRevC.73.034903 PACS number(s): 25.75.Ld

Directed flow in heavy-ion collisions is quantified by the first harmonic (v_1) in the Fourier expansion of the azimuthal distribution of produced particles with respect to the reaction plane [1]. It describes collective sideward motion of produced particles and nuclear fragments and carries information on the very early stages of the collision [2]. The shape of $v_1(y)$ in the

central rapidity region is of special interest because it might reveal a signature of a possible quark-gluon plasma (QGP) phase [3–5].

At AGS and SPS energies, v_1 versus rapidity is an almost linear function of rapidity [6–8]. Often just the slope of $v_1(y)$ at midrapidity is used to define the strength of directed flow. The sign of v_1 is by convention defined as positive for nucleons in the projectile fragmentation region. At these energies, the slope of $v_1(y)$ at midrapidity is observed to be positive for protons and significantly smaller in magnitude and negative for pions [6,7,9]. The opposite directed flow of pions is usually explained in terms of shadowing by nucleons. At Relativistic Heavy Ion Collider (RHIC) energies, directed flow is predicted to be smaller near midrapidity with a weaker dependence on pseudorapidity [10,11]. It may exhibit a characteristic wiggle [3,4,10,11], whereby directed flow changes sign three times outside the beam fragmentation regions, in contrast to the observed sideward deflection pattern at lower energies where the sign of $v_1(y)$ changes only once, at midrapidity. The observation of the slope of v_1 at midrapidity being negative for nucleons or positive for pions would constitute such a wiggle.

In one-fluid dynamical calculations [3,4], the wiggle structure appears only under the assumption of a QGP equation of state, thus becoming a signature of the QGP phase transition. Then the wiggle structure is interpreted to be a consequence of the expansion of the highly compressed, disk-shaped system, with the plane of the disk initially tilted with respect to the beam direction [3]. The subsequent system expansion leads to the so-called antiflow [3] or third flow component [4]. Such flow can reverse the normal pattern of sideward deflection as seen at lower energies and hence can result in either a flatness of v_1 or a wiggle structure if the expansion is strong enough. A similar wiggle structure in nucleon $v_1(y)$ is predicted if one assumes strong but incomplete baryon stopping together with strong space-momentum correlations caused by transverse radial expansion [10]. Although the predictions for baryon directed flow are unambiguous in both hydrodynamical and transport models, the situation for pion directed flow is less clear. RQMD model calculations [10] for Au+Au collisions at $\sqrt{s_{NN}} = 200$ GeV indicate that shadowing by protons causes the pions to flow mostly with opposite sign to the protons, but somewhat diffused because of higher thermal velocities for pions. Similar UrQMD calculations [11] predict no wiggle for pions in the central rapidity region with a negative slope at midrapidity as observed at lower collision energies.

At RHIC, most of the detectors cover the central rapidity region where the directed flow signal is small and the analysis procedures easily can be confused by azimuthal correlations not related to the reaction plane orientation, the so-called nonflow effects. Only recently have the first v_1 results been reported by the STAR Collaboration [12] and preliminary results by the PHOBOS Collaboration [13]. In Ref. [12], the shape of v_1 in the region on either side of midrapidity is poorly resolved because of large statistical errors. This shortcoming arose from having only about 70,000 events from the forward time projection chambers (FTPCs) [14] during their commissioning in the RHIC run II period (2002).

In this article, we present directed flow measurements in Au+Au collisions at $\sqrt{s_{NN}} = 62.4$ GeV. Results are obtained by three different methods, namely the three-particle cumulant method ($v_1\{3\}$) [15], the event-plane method with mixed harmonics ($v_1\{\mathrm{EP}_1, \mathrm{EP}_2\}$) [1,16], and the standard method [1] with the first-order event plane reconstructed from neutral fragments of the incident beams ($v_1\{\mathrm{ZDC\text{-}SMD}\}$). According to the standard method [1], directed flow can be evaluated by

$$v_1\{\mathrm{Standard}\} = \langle \cos(\phi - \Psi_1)\rangle / \mathrm{Res}(\Psi_1), \tag{1}$$

where ϕ and Ψ_1 denote the azimuthal angle of the particle and the first-order event plane, respectively, and $\mathrm{Res}(\Psi_1) = \langle \cos(\Psi_1 - \Psi_{\mathrm{RP}})\rangle$ represents the resolution of the first-order event plane. In the three-particle cumulant method [15], the flow is evaluated from

$$\begin{aligned}\langle\langle \cos(\phi_a + \phi_b - 2\phi_c)\rangle\rangle \equiv{}& \langle \cos(\phi_a + \phi_b - 2\phi_c)\rangle \\ &- \langle \cos(\phi_a + \phi_b)\rangle\langle \cos(-2\phi_c)\rangle \\ &- \langle \cos\phi_a\rangle\langle \cos(\phi_b - 2\phi_c)\rangle \\ &- \langle \cos\phi_b\rangle\langle \cos(\phi_a - 2\phi_c)\rangle \\ &+ 2\langle \cos\phi_a\rangle\langle \cos\phi_b\rangle\langle \cos(-2\phi_c)\rangle \\ ={}& v_{1,a} v_{1,b} v_{2,c},\end{aligned} \tag{2}$$

where on the r.h.s. of the first equality, the first term is a three-particle correlation and the other terms are to isolate the genuine three-particle correlation from spurious correlations induced by detector effects. Subscripts a, b, and c denote three different particles. This method was used in the first v_1 publication at RHIC [12]. The event plane method with mixed harmonics [16] utilizes the second-order event plane from the TPC, Ψ_2^{TPC}, and two first-order event planes from random subevents in the FTPCs, $\Psi_1^{\mathrm{FTPC}_1}$ and $\Psi_1^{\mathrm{FTPC}_2}$. It measures

$$v_1\{\mathrm{EP}_1, \mathrm{EP}_2\} = \frac{\left\langle \cos\left(\phi + \Psi_1^{\mathrm{FTPC}} + 2\Psi_2^{\mathrm{TPC}}\right)\right\rangle}{\sqrt{\left\langle \cos\left(\Psi_1^{\mathrm{FTPC}_1} + \Psi_1^{\mathrm{FTPC}_2} + 2\Psi_2^{\mathrm{TPC}}\right)\right\rangle \cdot \mathrm{Res}\left(\Psi_2^{\mathrm{TPC}}\right)}}, \tag{3}$$

where the emission angle of the particle ϕ is correlated with the first-order event plane Ψ_1^{FTPC} of the random subevent (made of tracks of both FTPCs) which does not contain the particle. $\mathrm{Res}(\Psi_2^{\mathrm{TPC}})$ represents the resolution of the second-order event plane measured in the TPC [16]. Both the cumulant method and the event plane method with mixed harmonics offer enhanced suppression of nonflow effects, including correlations because of momentum conservation, compared with the standard method (in which the event plane is reconstructed for the same harmonics and in the same rapidity region where the event anisotropy is measured). In the present study, the procedures to obtain $v_1\{3\}$ and $v_1\{\mathrm{EP}_1, \mathrm{EP}_2\}$ are essentially the same as in Ref. [12]. In the third method, the reaction plane was determined from the sideward deflection of spectator neutrons ("bounce-off") [8] measured in the zero-degree calorimeters (ZDCs) [17]. This is the first report from RHIC of flow results with the event plane reconstructed from spectator fragments. Five million minimum-bias events were used in this study for each of the three analyses, and all the errors presented are statistical. Cuts used in the TPC ($|\eta| < 1.3$) [18] and FTPC ($2.5 < |\eta| < 4.0$) analyses are the same as listed in Table II of Ref. [16], except that the vertex z cut is from -30 to 30 cm. The centrality definition, based on the raw charged

TABLE I. The resolution of the first-order event plane [1] provided by the ZDC-SMDs, as determined from the subevent correlation between east and west SMDs. The errors in the table are statistical.

Centrality	Event-plane resolution
70–80%	0.179 ± 0.005
60–70%	0.185 ± 0.004
50–60%	0.176 ± 0.005
40–50%	0.167 ± 0.005
30–40%	0.138 ± 0.006
20–30%	0.110 ± 0.008
10–20%	0.081 ± 0.010

particle TPC multiplicity with $|\eta| < 0.5$, is the same as used previously [16].

In the fall of 2003, STAR installed shower maximum detectors (SMDs) sandwiched between the first and second modules of each existing STAR ZDC at $|\eta| > 6.3$. Each SMD consists of two plastic scintillator planes, one of seven vertical slats and another of eight horizontal slats. The two SMDs provide event-by-event information on the transverse distribution of energy deposition of the spectator neutrons. The weighted center of the energy distribution determines the event plane vector on each side. The combination of the east and west event plane vectors provides the full event plane and the event-plane resolution is obtained from the correlation of the two event plane vectors in the standard way. The $v_1\{\text{ZDC-SMD}\}$ should have minimal contribution from nonflow effects because of the large rapidity gap between the spectator neutrons used to establish the reaction plane and the rapidity region where the measurements were performed. The resolution, as defined in Ref. [1], of the first-order event plane reconstructed using the ZDC-SMDs is listed in Table I.

The centrality ranges of Au+Au collisions at $\sqrt{s_{NN}} = 62.4$ GeV where the three v_1 methods work are slightly different: $v_1\{3\}$ fails at centralities less than 5% and centralities greater than 70%, because the four-particle cumulant $v_2\{4\}$, which is a necessary ingredient for measuring $v_1\{3\}$, is not measurable in those regions possibly because of large v_2 fluctuations; $v_1\{\text{ZDC-SMD}\}$ fails for centrality less than 10% because of insufficient event-plane resolution in central collisions. Figure 1 shows charged particle v_1 as a function of pseudorapidity, η, for centrality 10–70% where all three methods work, from Au+Au collisions at $\sqrt{s_{NN}} = 62.4$ GeV. The arrows in the upper panel indicate the direction of flow for spectator neutrons as determined from the ZDC-SMDs. The lower panel shows on expanded scales the midpseudorapidity region measured by the STAR TPC. The results from the three different methods agree with each other very well. In Ref. [12], the relative systematic uncertainty in $v_1\{3\}$ and $v_1\{\text{EP}_1, \text{EP}_2\}$ was estimated to be about 20%. That error estimate was obtained under the assumption that the directed flow measurements using two-particle correlations were totally dominated by nonflow effects. Such an assumption provides an upper limit on the systematic errors. Reference [16] provides further discussion on the systematic uncertainties. The comparison

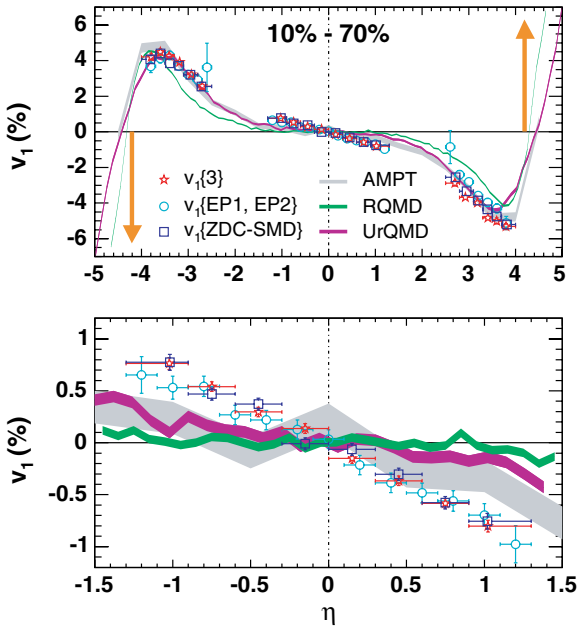

FIG. 1. (Color online) Directed flow of charged particles as a function of pseudorapidity, for centrality 10–70%. The arrows in the upper panel indicate the direction of flow for spectator neutrons. The arrow positions on the pseudorapidity axis corresponds to where the incident ions would lie on a rapidity scale. The lower panel shows the midpseudorapidity region in more detail. The plotted errors are statistical only, and systematic effects are discussed in the text.

of $v_1\{\text{ZDC-SMD}\}$ and $v_1\{3\}$ indeed shows that the relative difference is no more than 20% around midpseudorapidity (where the directed flow itself is less than 0.005) and the difference is only about 5% in the forward pseudorapidity region. $v_1\{\text{ZDC-SMD}\}$ was also calculated using the information from the east and west ZDCs separately as well as separately from correlations in the vertical and horizontal directions (note that the ZDC-SMDs have a rectangular shape); all the results agree within 15%. In another systematic study of $v_1\{\text{ZDC-SMD}\}$, a tighter distance of the closest approach (dca) cut was applied to reduce the number of weak decay tracks or secondary interactions. The ratio of v_1 obtained with dca <1 cm to the v_1 result with the default cut (dca <2 cm) was measured to be $v_1^{\text{dca}<1\,\text{cm}}/v_1^{\text{dca}<2\,\text{cm}} = 1.00 \pm 0.07$ for charged particles.

AMPT [19], RQMD [2], and UrQMD [20] model calculations for the same centrality of Au+Au collisions at $\sqrt{s_{NN}} = 62.4$ GeV are also shown in Fig. 1. Most transport models, including AMPT, RQMD, and UrQMD, underpredict elliptic flow (v_2) at RHIC energies, and we now report that they also underpredict the charged particle $v_1(\eta)$ within a unit or so of midpseudorapidity but then come into good agreement with the data over the region $2.5 < |\eta| < 4.0$. Although the magnitude of v_1 for charged particles increases with the magnitude of pseudorapidity below $|\eta| \sim 3.8$ for centralities between 10 and 70%, our results are compatible with the peak in $|v_1|$ lying in the $|\eta|$ region predicted by all three models, namely 3.5 to 4.0.

No apparent wiggle structure, as discussed above, is observed within our acceptance. Throughout our pseudorapidity acceptance, charged particles on a given side of $\eta = 0$ flow

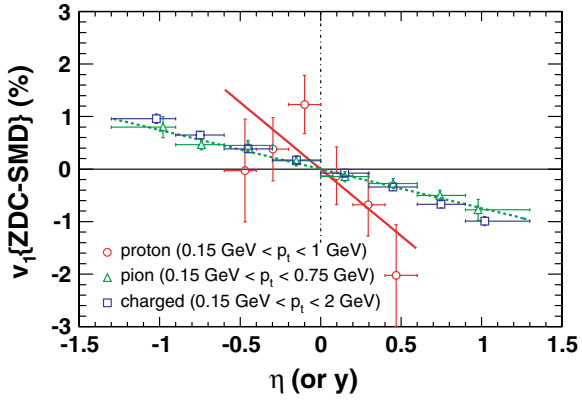

FIG. 2. (Color online) v_1 versus rapidity for protons and pions. The charged particle $v_1(\eta)$ is plotted as a reference. The different upper end of the p_t range for protons and pions is because of different limits of the dE/dx identification method. The solid and dashed lines are results from linear fits described in the text. All results are from analyses using the reaction plane reconstructed by the ZDC-SMD, v_1{ZDC-SMD}. The plotted errors are statistical only, and systematic effects are discussed in the text.

in the opposite direction to the fragmentation neutrons on that side. This is consistent with the direction expected in the "antiflow" scenario [3] but it is also the same direction as measured for pions at lower energies that is usually related to the pion shadowing by nucleons. Assuming that the charged particle flow at beam rapidity is dominated by protons, one would conclude that over the entire pseudorapidity range $v_1(\eta)$ changes sign three times. However, this does not prove the existence of the wiggle structure for protons and pions separately. Measurements of directed flow of identified particles could be more informative in this respect. In STAR, particle identification is feasible only in the main TPC, which covers the pseudorapidity region $|\eta| < 1.3$. In this region, the RQMD model predicts very flat $v_1(\eta)$ for pions and a clear wiggle structure, with negative slope $dv_1/d\eta$ at midpseudorapidity for protons at $\sqrt{s_{NN}} = 62.4$ GeV. (The relatively strong wiggle for pions reported in Ref. [10] is developed only at higher collision energies.) To maximize the magnitude of the possible slope, we select the centrality interval 40 to 70%, where flow anisotropies normally are at their peak. The result is shown in Fig. 2. With the current statistics, we observe that pion flow is very similar to that of charged particles, with the slope at midrapidity dv_1/dy about -0.0074 ± 0.0010, obtained from a linear fit over the region $|y| < 1.3$ (dashed line). For protons, the slope dv_1/dy is -0.025 ± 0.011 from a linear fit in $|y| < 0.6$ (solid line). At present, STAR's statistics for baryons are rather small compared with the statistics for all charged particles, and our best estimates of the fitted slope are such that a negative baryon slope with comparable magnitude to the RQMD prediction is not decisively ruled out. For the identified particles, the influence of the particle identification procedures on the flow values for pions and protons may be a source of errors. By default we eliminate particles 3σ away from the expected TPC energy loss for the relevant particle type. When we tightened the cut to 2σ instead of 3σ, we found that for 40–70% most central events, the v_1{ZDC-SMD} of pions is reduced by less than

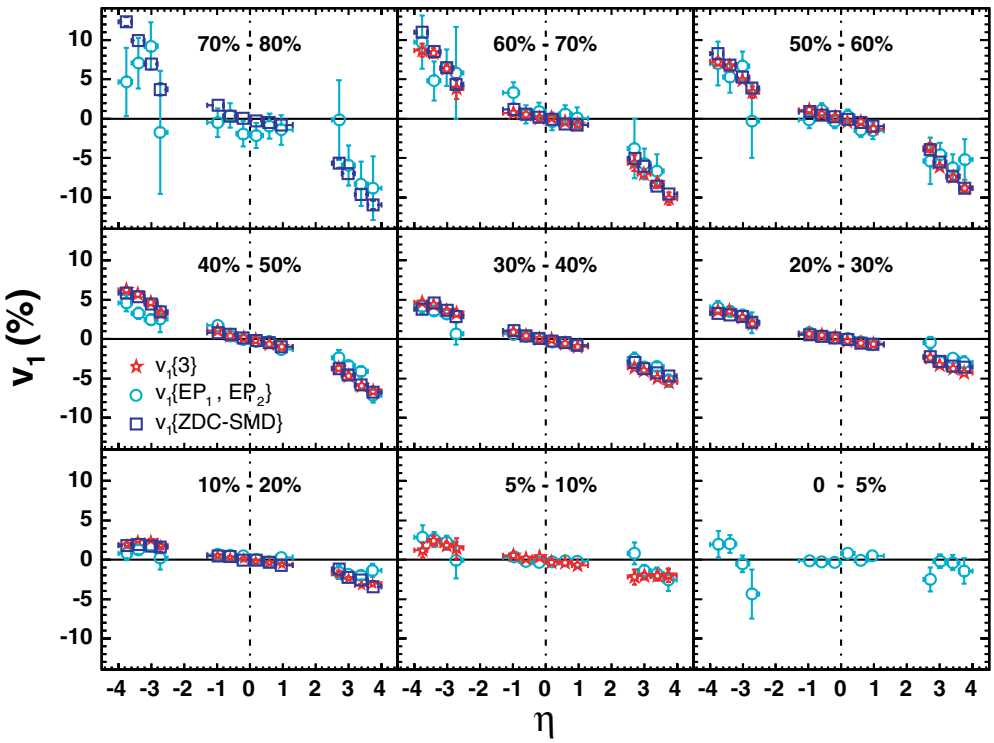

FIG. 3. (Color online) Directed flow of charged particles as a function of pseudorapidity for different centralities. The plotted errors are statistical.

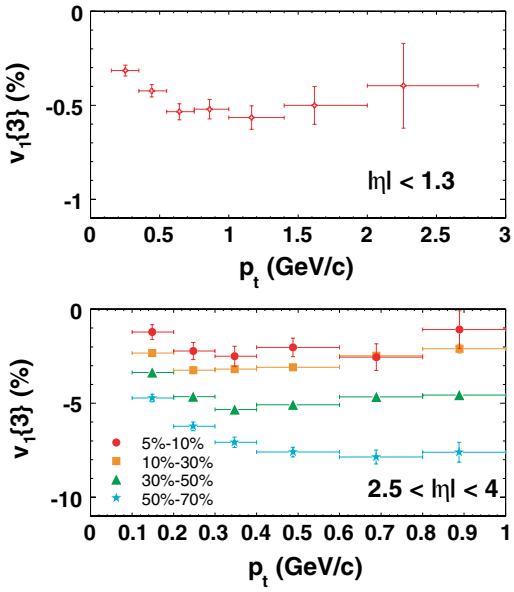

FIG. 4. (Color online) The upper panel shows $v_1\{3\}$ versus p_t measured in the main TPC ($|\eta| < 1.3$), for centrality 10–70%. The lower panel shows $v_1\{3\}$ versus p_t measured by the TPC ($2.5 < |\eta| < 4.0$) for different centralities. Note the different scales on both axes for the two panels. The differential directed flow of particles with negative η has been changed in sign as stated in the text. The plotted errors are statistical.

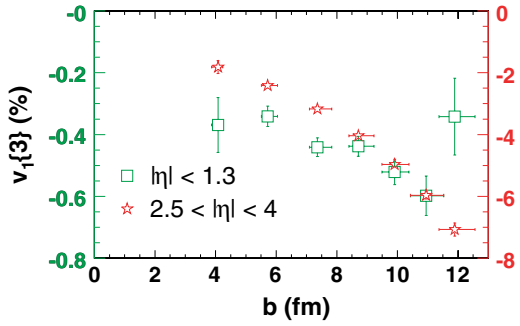

FIG. 5. (Color online) Directed flow of charged particles as a function of impact parameter for the midpseudorapidity region ($|\eta| < 1.3$, with the left vertical scale) and the forward pseudorapidity region ($2.5 < |\eta| < 4.0$, with the right vertical scale). The differential directed flow of particles with negative η has been changed in sign as stated in the text. The plotted errors are statistical.

10%, whereas the proton $v_1\{\text{ZDC-SMD}\}$ stays constant within errors.

Figure 3 shows v_1 of charged particles as a function of η for different centralities. We do not observe an onset of any special feature in the pseudorapidity dependence of v_1 at any centrality. Preliminary $v_1(\eta)$ results from PHOBOS [21] for centrality 0 to 40% are consistent with our data at the same centrality except that $|v_1(\eta)|$ from PHOBOS has its peak at $|\eta|$ of about 3 to 3.5, whereas STAR's $|v_1(\eta)|$ peaks at $|\eta|$ about 3.8 or higher. A significant change in particle abundances below STAR's transverse-momentum acceptance cut (0.15 GeV/nucleon), might account for some or all of this difference in the $|v_1|$ peak position.

The transverse-momentum dependence of v_1 is shown in Fig. 4. Because $v_1(\eta, p_t)$ is asymmetric about $\eta = 0$, the integral of $v_1(\eta, p_t)$ over a symmetric η range goes to zero. We change $v_1(\eta, p_t)$ of particles with negative η into $-v_1(-\eta, p_t)$ and integrate over all η. because of the small magnitude of the v_1 signal close to midpseudorapidity ($|\eta| < 1.3$), only the averaged $v_1(p_t)$ over centralities 10–70% is shown. For $2.5 < |\eta| < 4.0$, the v_1 signal is large enough to be resolved for different centrality regions. The poor p_t resolution for higher p_t in FTPCs limits the p_t range to below 1 GeV/nucleon for $2.5 < |\eta| < 4.0$. For all centralities and pseudorapidity regions, the magnitude of v_1 is observed to reach its maximum at $p_t \approx 1$ GeV/nucleon for $|\eta| < 1.3$ and at $p_t \approx 0.5$ GeV/nucleon for $2.5 < |\eta| < 4.0$. Note that from its definition, $v_1(p_t)$ must approach zero as p_t approaches zero. The centrality dependence of p_t-integrated v_1 is shown in Fig. 5. The values of the impact parameter were obtained using a Monte Carlo Glauber calculation [22], listed in Table II. As expected, v_1 decreases with centrality. It is seen that v_1 in the more forward pseudorapidity region $2.5 < |\eta| < 4.0$ varies more strongly with centrality than in the region closer to midpseudorapidity ($|\eta| < 1.3$).

It has been observed that particle emission (both spectra and flow) as a function of rapidity distance from beam rapidity appears unchanged over a wide range of beam energies [12,23,24], a pattern known as limiting fragmentation [25]. Figure 6 presents v_1 results in the projectile frame for three beam energies. In this frame, zero on the horizontal axis corresponds to beam rapidity for each of the three beam energies. The data support the limiting fragmentation hypothesis in the region $-2 < y - y_{\text{beam}} < -1$.

In summary, we have presented the first measurements of charged particle directed flow in Au+Au collisions at $\sqrt{s_{NN}} = 62.4$ GeV. The analysis has been performed using three different methods and the results agree very well with each other. One of the methods involves the determination of the reaction plane from the bounce-off of fragmentation neutrons, the first measurement of this type at RHIC. This method provides measurements of directed flow that are expected to have negligible systematic uncertainty arising from nonflow effects. In addition, these measurements provide a

TABLE II. The correspondence between centrality and impact parameter.

Centrality	Impact parameter (fm)
70–80%	$12.82 + 0.62 - 0.67$
60–70%	$11.89 + 0.67 - 0.52$
50–60%	$10.95 + 0.58 - 0.52$
40–50%	$9.91 + 0.47 - 0.42$
30–40%	$8.71 + 0.52 - 0.31$
20–30%	$7.36 + 0.47 - 0.26$
10–20%	$5.72 + 0.32 - 0.21$
5–10%	$4.08 + 0.16 - 0.21$
0–5%	$2.24 + 0.07 - 0.14$

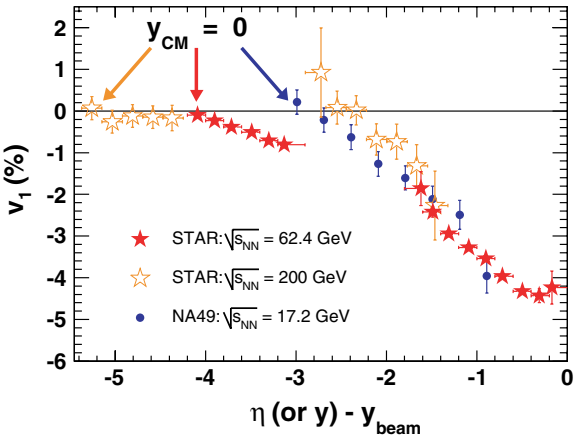

FIG. 6. (Color online) Charged particle v_1 for Au+Au collisions (10–70%) at 200 GeV [12] (open stars) and 62.4 GeV (solid stars), as a function of $\eta - y_{\text{beam}}$. Also shown are results from NA49 [7] (circles) for pions from 158A GeV midcentral (12.5–33.5%) Pb+Pb collisions as a function of $y - y_{\text{beam}}$. The 62.4- and 200-GeV points are averaged over the positive and negative rapidity regions. All results are from analyses involving three-particle cumulants, $v_1\{3\}$. The plotted errors are statistical.

determination of the sign of v_1. In this way, we conclude that charged particles in the pseudorapidity region covered by the STAR TPC and FTPCs (up to $|\eta| = 4.0$) flow in the opposite direction to the fragmentation nucleons with the same sign of η. The p_t-dependence of v_1 saturates above $p_t \approx 1$ GeV/nucleon in the midpseudorapidity region and $p_t \approx 0.5$ GeV/nucleon in the forward pseudorapidity region. Over the pseudorapidity range studied, no sign change in the slope of charged-particle v_1 versus pseudorapidity is observed at any centrality. The centrality dependence of v_1 in the region of $2.5 < |\eta| < 4.0$ is found to be stronger than what is observed closer to midpseudorapidity. The rapidity dependence of v_1 provides further support for the limiting fragmentation picture.

ACKNOWLEDGMENTS

We thank Sebastian White for consultations and help in construction of the STAR ZDC-SMD, and we acknowledge the RHIC Operations Group and RCF at BNL and the NERSC Center at LBNL for their support. This work was supported in part by the HENP Divisions of the Office of Science of the U.S. DOE; the U.S. NSF; the BMBF of Germany; IN2P3, RA, RPL, and EMN of France; EPSRC of the United Kingdom; FAPESP of Brazil; the Russian Ministry of Science and Technology; the Ministry of Education and the NNSFC of China; IRP and GA of the Czech Republic; FOM of the Netherlands; DAE, DST, and CSIR of the Government of India; Swiss NSF; the Polish State Committee for Scientific Research; STAA of Slovakia; and the Korea Sci. & Eng. Foundation.

[1] A. M. Poskanzer and S. A. Voloshin, Phys. Rev. C **58**, 1671 (1998).
[2] H. Sorge, Phys. Rev. Lett. **78**, 2309 (1997).
[3] J. Brachmann, S. Soff, A. Dumitru, H. Stocker, J. A. Mahruhn, W. Greiner, L. V. Bravina, and D. H. Rischke, Phys. Rev. C **61**, 024909 (2000).
[4] L. P. Csernai and D. Röhrich, Phys. Lett. **B458**, 454 (1999).
[5] H. Stöcker, Nucl. Phys. **A750**, 121 (2005).
[6] E877 Collaboration, J. Barrette *et al.*, Phys. Rev. C **55**, 1420 (1997); J. Barrette *et al.*, Phys. Rev. C **56**, 3254 (1997).
[7] NA49 Collaboration, C. Alt *et al.*, Phys. Rev. C **68**, 034903 (2003).
[8] W. Reisdorf and H. G. Ritter, Annu. Rev. Nucl. Part. Sci. **47**, 663 (1997); N. Herrmann, J. P. Wessels, and T. Wienold, Annu. Rev. Nucl. Part. Sci. **49**, 581 (1999).
[9] WA98 Collaboration, M. M. Aggarwal *et al.*, nucl-ex/9807004.
[10] R. J. M. Snellings, H. Sorge, S. A. Voloshin, F. Q. Wang, and N. Xu, Phys. Rev. Lett. **84**, 2803 (2000).
[11] M. Bleicher and H. Stöcker, Phys. Lett. **B526**, 309 (2002).
[12] STAR Collaboration, J. Adams *et al.*, Phys. Rev. Lett. **92**, 062301 (2004).
[13] M. Belt Tonjes, for PHOBOS Collaboration, B. B. Back *et al.*, J. Phys. G **30**, S1243 (2004).
[14] K. H. Ackermann *et al.*, Nucl. Instrum. Methods A **499**, 713 (2003).
[15] N. Borghini, P. M. Dinh, and J.-Y. Ollitrault, Phys. Rev. C **66**, 014905 (2002).
[16] STAR Collaboration, J. Adams *et al.*, Phys. Rev. C **72**, 014904 (2005).
[17] C. Adler *et al.*, Nucl. Instrum. Methods A **470**, 488 (2001); The STAR ZDC-SMD has the same structure as the STAR EEMC SMD: C. E. Allgower *et al.*, *ibid.* **499**, 740 (2003); STAR ZDC-SMD proposal, STAR Note SN-0448 (2003).
[18] M. Anderson *et al.*, Nucl. Instrum. Methods A **499**, 659 (2003).
[19] Z.-W. Lin and C. M. Ko, Phys. Rev. C **65**, 034904 (2002); L.-W. Chen and C. M. Ko, J. Phys. G **31**, S49 (2005); L.-W. Chen (private communication).
[20] S. A. Bass *et al.*, Prog. Part. Nucl. Phys. **41**, 225 (1998); M. Bleicher *et al.*, J. Phys. G **25**, 1859 (1999); X.-L. Zhu (private communication).
[21] PHOBOS Collaboration, B. Alver *et al.*, nucl-ex/0510030.
[22] PHOBOS Collaboration, B. B. Back *et al.*, Phys. Rev. C **65**, 031901(R) (2002);PHENIX Collaboration, K. Adcox *et al.*, Phys. Rev. Lett. **86**, 3500 (2001); BRAHMS Collaboration, I. G. Bearden *et al.*, Phys. Lett. **B523**, 227 (2001); STAR Collaboration, J. Adams *et al.*, nucl-ex/0311017.
[23] PHOBOS Collaboration, B. B. Back *et al.*, Phys. Rev. Lett. **91**, 052303 (2003); **94**, 122303 (2005).
[24] STAR Collaboration, J. Adams *et al.*, Phys. Rev. Lett. **95**, 062301 (2005).
[25] J. Benecke, T. T. Chou, C.-N. Yang, and E. Yen, Phys. Rev. **188**, 2159 (1969).